

This is the Author's Post-print version of the following article: *V. Ibarra-Junquera, J.S. Murguía, P. Escalante-Minakata, H.C. Rosu, Application of multifractal wavelet analysis to spontaneous fermentation processes, Physica A: Statistical Mechanics and its Applications, Volume 387, Issue 12, 2008, Pages 2802-2808*, which has been published in final form at <https://doi.org/10.1016/j.physa.2008.01.083> This article may be used for non-commercial purposes in accordance with Terms and Conditions for Self-Archiving

Application of Multifractal Wavelet Analysis to Spontaneous Fermentation Processes

V. Ibarra-Junquera ^a,
J.S. Murguía ^b, P. Escalante-Minakata ^a, H.C. Rosu ^c

^a*Faculty of Chemical Sciences, University of Colima, Coquimatlán, Col., Mexico*

^b*DFM-UASLP, San Luis Potosí, S.L.P., Mexico*

^c*Division of Advanced Materials, IPICYT, San Luis Potosí, S.L.P., Mexico*

Physica A (2008)

doi: 10.1016/j.physa.2008.01.083

arXiv: 0710.2362 v2; multifr1.tex

Abstract

An algorithm is presented here to get more detailed information, of mixed culture type, based exclusively on the biomass concentration data for fermentation processes. The analysis is performed with only the on-line measurements of the redox potential being available. It is a *two-step* procedure which includes an Artificial Neural Network (ANN) that relates the redox potential to the biomass concentrations in the first step. Next, a multifractal wavelet analysis is performed using the biomass estimates of the process. In this context, our results show that the redox potential is a valuable indicator of microorganism metabolic activity during the spontaneous fermentation. In this paper, the detailed design of the multifractal wavelet analysis is presented, as well as its direct experimental application at the laboratory level.

Key words: Multifractal; Wavelet; Mixed-culture; Spontaneous fermentation; Redox potential

Email addresses: vij@ucol.mx (V. Ibarra-Junquera), ondeleto@uaslp.mx (J.S. Murguía), minakata@ipicyt.edu.mx (P. Escalante-Minakata), hcr@ipicyt.edu.mx (H.C. Rosu).

1 Introduction

During spontaneous fermentation processes, microorganisms employ sugars and other constituents of must as substrate for their growth, converting them into ethanol, carbon dioxide, higher alcohols and their esters, and other metabolic compounds. In general, it could be useful to know more about the dynamics of the entire microflora during spontaneous fermentations. In particular, an analysis that enables a monitoring process could be fundamental for a quality control that ensures at least the homogeneity of the final product.

Nevertheless, a bottleneck in all biochemical monitoring process is often the lack of sensors for biological variables. Moreover, it is a well-known issue that in order to monitor many biotechnological processes, the problem of growth rate estimations represent a strategic feature. Previously, various attempts of relating the *redox potential* to fermentation processes have been made taking into account that *redox potential* assesses the growth ability of microorganisms, as well as the physiological activity in a given environment [2], [3], [4], [5]. Particularly, the practical significance of redox potential and oxygen content at various stages of winemaking was examined in [6]. Many chemical, enzymatic and biological processes in wine are correlated with the oxidative state of the wine.

It is well known that many natural systems exhibit complex dynamics described by long-range power laws. In some cases the output of such systems, which corresponds to a fluctuating time series, may be characterized or quantified by a spectrum of exponents called the multifractal spectrum. The multifractal formalism to characterize processes, measures, and functions, introduced by Halsey and collaborators [7], opened a new direction for the search of dimension type characteristics of dynamical systems in the form of spectra for dimensions that reflect both the geometric and dynamical structure of nonlinear systems. Despite the fact that there are a variety of methods to calculate the singularity spectrum of a multifractal structure, the method based upon the wavelet theory appears to be the most appealing and successful [8]. In fact, the interest in wavelet methods is that they are numerically more stable [9]. In 1993, Bacry *et al.* [10] developed this method based on the definition of a partition function in which the concept of wavelet transform modulus maxima (WTMM) was implemented. They demonstrated that the singularity spectrum for a Bernoulli measure or a fractal distribution can be readily determined from the scaling behavior of such a partition function and similar results have been proved for more general measures by Murguía and Urías [11].

The paper is organized as follows. Section 2 is devoted to a concise presentation of the fermentation experiment performed to illustrate our approach. The data

analysis, which is a combination of an ANN and a multifractal wavelet scheme, is described in Section 3. Finally, the paper ends up with some concluding remarks.

2 Experimental setup

2.1 *Microorganism and culture conditions*

In order to evaluate experimentally how suitable the estimation algorithm is, we performed six individual batch experiments with the must of *Agave* (or *Agave* syrup) for which we used inocula of native microorganisms (without the addition of any commercial strain). This must was centrifuged at $8000\text{ rpm} \times 10\text{ min}$ and stored in a frozen state at -20°C prior to experiments.

The batch fermentations were carried out in a bioreactor with pH and redox sterilizable electrodes. The electrodes are connected to a console for data acquisition, a device which is connected to a computer where the data are stored and computed as can be seen in Fig. 1.

The bioreactor was filled with 900 mL of must as a culture medium, 100 mL of the inoculum in its exponential growing phase (biomass 0.1 g/L) and 0.1% of ammonium sulfate at final concentration. The initial conditions of the fermentation were settled at a temperature of 32.5°C and initial sugar concentration of 70 g/L . The pH does not show a dynamic evolution, maintaining itself at a value of 4 during the whole process.

2.2 *Analytical procedures and measurements*

The batch processes have been monitored for 14 hours, through sampling under sterile conditions. In order to quantify biomass and ethanol concentrations, 5 mL samples of culture were removed every 30 min . The samples were cleared by centrifugation at 6000 rpm for 5 minutes at room temperature. The next step was to collect the supernatant phase and store it frozen at -20°C prior to be analyzed. The obtained pellet was resuspended in distilled water in order to proceed with the biomass analysis.

The biomass measurements have been performed using (varian) UV spectroscopy at 600 nm . The obtained values were interpolated with a standard curve of cell dry weight concentration.

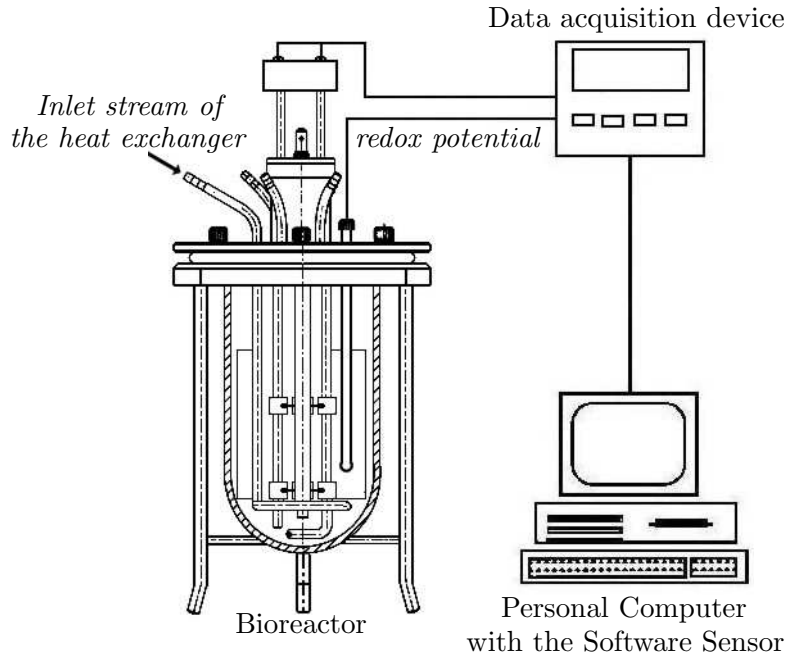


Fig. 1. The schematic representation of the experiments carried out in our laboratory.

2.3 Redox potential

The measurement of *redox potential* is relatively fast, accurate, and reliable and its values give an insight into the oxidation process as well as the inherent ability of reduction in the process, which is well established in the case of wine [6]. The measured values of the *redox potential* can give information on redox reactions in wine, which have an important effect on its quality and stability [6]. During storing and aging of wine, oxidation and reduction processes affect the character and taste of wine to a considerable extent [6], [5]. In our *Agave* case, the *redox potential* measurements were acquired periodically each 0.01 *hr* during 14 *hrs*, and the data were stored and processed on line by means of a computer (see Fig. 1).

3 Data analysis

3.1 Artificial neural network

In order to relate the redox measurements to the biomass concentration an ANN procedure is applied. The methodology that we carried out includes a forward-propagation training algorithm for the ANN using some of our experimental data. In order to perform our task we construct a model of the

following form:

$$X_1 = g(X_2) \tag{1}$$

where X_2 represents the *redox potential* measurement data (mV), $X_1 = F(t)$ is the set of time-dependent biomass concentration data (mg/L) and the function $g(X_2)$ is approximated by means of the ANN procedure. The ANN architecture is of the standard type [12] with a single ANN hidden-layer containing 10 units.

Each unit of this network uses a sigmoid function as the activation function. On the other hand, the output contains a linear activation function, in our case the identity. The feed-forward training algorithm considered here is the conjugate gradient method [13]. Three of the six individual batch experiments were used to provide data for the training process. The ANN after the training gives an error of only 0.0029.

3.2 Multifractal wavelet analysis

The *wavelet transform* (WT) of a distribution function $s(t)$ is given by

$$W_s(a, b) = \frac{1}{a} \int_{-\infty}^{\infty} s(t) \bar{\psi} \left(\frac{t-b}{a} \right) dt, \tag{2}$$

where ψ is the analyzing wavelet, $b \in \mathbb{R}$ is a translation parameter, whereas $a \in \mathbb{R}^+$ ($a \neq 0$) is a dilation or scale parameter, and the bar symbol denotes complex conjugation.

One fundamental property that we require in order to analyze singular behavior is that $\psi(t)$ has enough vanishing moments [10,14]. A wavelet is said to have n vanishing moments if and only if it satisfies

$$\int_{-\infty}^{\infty} t^k \psi(t) dt = 0, \quad \text{for } k = 0, 1, \dots, n-1, \tag{3}$$

and

$$\int_{-\infty}^{\infty} t^k \psi(t) dt \neq 0, \quad \text{for } k = n. \tag{4}$$

This means that a wavelet with n vanishing moments is orthogonal to all polynomials up to order $n-1$. So the wavelet transform of $s(t)$ with a wavelet

$\psi(t)$ with n vanishing moments is nothing but a “smoothed version” of the n th derivative of $s(t)$ on various scales.

In the presence of a singularity in the data at a particular point t_0 , the scaling behavior of the wavelet coefficients is described by the Hölder exponent $\alpha(t_0)$ as

$$W_s(a, t_0) \sim a^{\alpha(t_0)}, \quad (5)$$

in the limit $a \rightarrow 0^+$.

The continuous wavelet transform given in Eq. 2 is an extremely redundant representation, too costly for most practical applications. To characterize the singular behavior of functions, it is sufficient to consider the values and position of the WTMM [14]. The latter is a point (a_0, b_0) on the scale-time plane, (a, b) , where $|W_s(a_0, b)|$ is locally maximum for b in the neighborhood of b_0 . These maxima are located along curves in the plane (a, b) . However, the relationship (5) in some cases is not appropriated to describe distribution functions with non-isolated singularities. The wavelet multifractal formalism may characterize fractal objects which cannot be completely described by a single fractal dimension. According to Bacry *et al.* [10], an “optimal” partition function $\mathcal{Z}_q(s, a)$ can be defined in terms of the WTMM. They consider the set of modulus maxima at a scale a as a covering of the singular support of s with wavelets of scale a . The partition function \mathcal{Z}_q measures the sum of all wavelet modulus maxima at a power q as follows

$$\mathcal{Z}_q(s, a) = \sum_p |W_s(a, b_p(a))|^q, \quad (6)$$

where $\{b_p(a)\}_{p \in \mathbb{Z}}$ is the position of all local maxima of $|W_s(a, b)|$ at a fixed scale a . This partition function is very close to the definition of the partition function described in [7]. It can be inferred from (6) that for $q > 0$ the most pronounced modulus maxima will prevail, whereas for $q < 0$ the lower ones will survive. For each $q \in \mathbb{R}$, the partition function is related to the scaling exponent $\tau(q)$ in the following way $\mathcal{Z}_q(s, a) \sim a^{\tau(q)}$. A linear behavior of $\tau(q)$ indicates monofractality whereas nonlinear behavior indicates a multifractal signal. A fundamental result in the (wavelet) multifractal formalism states that the singularity (Hölder) spectrum $f(\alpha)$ of the distribution function $s(t)$ is the Legendre transform of $\tau(q)$, i.e.,

$$\alpha = \tau'(q), \quad \text{and} \quad f(\alpha) = q\alpha - \tau(q). \quad (7)$$

The Hölder spectrum of dimensions $f(\alpha)$ is a nonnegative convex function that is supported on the closed interval $[\alpha_{\min}, \alpha_{\max}]$, which is interpreted as the

Hausdorff fractal dimension of the subset of data characterized by the Hölder exponent α [11]. The most “frequent” singularity, which corresponds to the maximum of $f(\alpha)$, occurs at the value of $\alpha(q = 0)$, whereas the boundary values of the support, α_{\min} for $q > 0$ and α_{\max} for $q < 0$, correspond to the strongest and weakest singularity, respectively.

The analyzing wavelets which are used most frequently are the successive derivatives of the Gaussian function

$$\psi^{(n)}(t) := \frac{d^n}{dt^n} \left(\exp(-t^2/2) \right), \quad n \in \mathbb{Z}^+, \quad (8)$$

because they are well localized both in space and frequency, and they remove the signal trends that can be approximated by polynomials up to the $(n - 1)$ th order [9]. In particular, our analysis was carried out with the Mexican hat wavelet $\psi^{(2)}(t)$.

4 Results and discussion

We performed the multifractal wavelet analysis based on the WTMM method employing the biomass ANN estimates for two *Agave* spontaneous fermentation processes. For the first one, we present the reconstructed biomass signal and the redox experimental signal in Fig. (2) (a,b), respectively. In general, for extracting the singularity structure of a signal according to wavelet transform techniques one should get the modulus maxima lines of the (continuous) wavelet transform. These are displayed in Fig. (2) (c,d) and one can immediately notice that for both reconstructed and real experimental redox data we do not obtain isolated singularities as those treated in our previous work [1], on the contrary there is a high density of singularities. This fact induces us to think of the multifractal formalism which could be more appropriate in such cases. The complete evidence of the multifractal character of the signals is a scaling exponent τ with two different slopes, where the point of bending in the $\tau(q)$ spectrum is directly related to the most frequent singularity of the biomass data. It is worth noting that the locations of the maxima lines are almost the same for both the reconstructed biomass data and the direct experimental redox potential data, see the same figure (e). This indicates that the effect of the ANN procedure on the singularity structure of the redox signal is small and that we can be confident in the ANN-based total biomass estimates. Thus, assuming that these spontaneous phenomena are multifractal processes, we calculated in Fig. (2) (f,g) the two basic multifractal quantities, namely the $\tau(q)$ and $f(\alpha)$ spectra for both sets of data. We confirm the multifractality of both signals since we indeed get a τ spectrum with two slopes in both cases. The support of the singularity spectrum for the biomass signal

is $\alpha \in [0.11, 1.36]$ with the maximum of the spectrum located at $\alpha_{peak} = 0.95$ that gives us the most frequent singularity $f_B(\alpha_{peak}) = 0.756$, whereas in the case of the redox potential we get the support $\alpha \in [0.1, 1.04]$ with $\alpha_{peak} = 0.984$ giving the most frequent singularity $f_R(\alpha_{peak}) = 0.588$.

We repeated the same multifractal analysis for another data set of the *Agave* spontaneous fermentation process to examine the reproduction of our results of the previous case. The second analysis is displayed in Fig. (3). We again get the confirmation of the multifractal behaviour from the two-sloped τ spectrum, but of course as we deal with a different time series we have slightly different multifractal parameters. The support of the singularity spectrum for the biomass signal is now $\alpha \in [0.188, 1.38]$ with the maximum of the spectrum located at $\alpha_{peak} = 0.84$ providing as the most frequent singularity $f_B(\alpha_{peak}) = 0.68$, whereas in the case of the redox potential we get now the support $\alpha \in [0.1, 0.88]$ with $\alpha_{peak} = 0.7885$ that gives for the most frequent singularity the value $f_R(\alpha_{peak}) = 0.633$.

There is still one point to discuss, which is why the Hölder support extends up to one for the experimental redox potential signal whereas it goes substantially beyond one in the case of the biomass signal in the two cases. We have found in the literature that a similar situation has been encountered by Humeau and collaborators [15] in the case of the laser Doppler flowmetry signals. The Hölder exponents of their simulated data are greater than one as compared to their real signals for which they are less than one. They comment that in general the simulated data are smoother whereas the real signals are much more irregular.

5 Conclusions

Although mixtures of microorganisms may look natural in fermentation processes, the total biomass, which is the quantity most easy to deal with, does not provide definite evidence for the mixture by itself. However, in such processes the redox potential and the total biomass concentration are related fluctuating quantities thence the redox potential signal may contain relevant information on the microorganism metabolisms. This can be inferred through the multifractal techniques which has been specially designed for signals with significant irregular contributions.

The main finding of this paper is that the spontaneous fermentation processes in the case of the *Agave* syrup can be characterized as a multifractal process and that the Hölder exponents are a good measure of the degree of irregularity of the signals. Since the total biomass concentration and the redox potential signals are connected spontaneous time series we expect to get quite similar

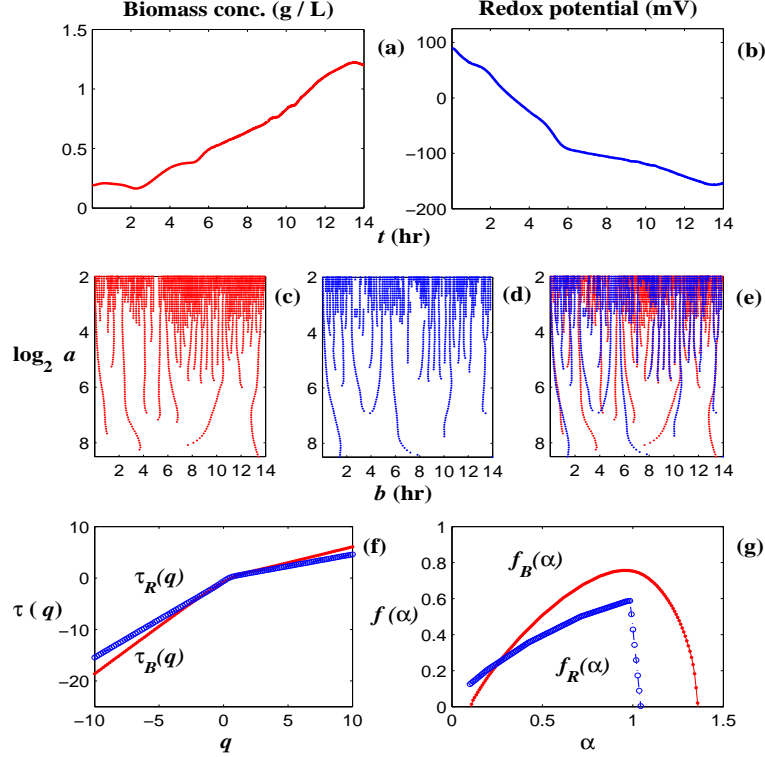


Fig. 2. (a) Biomass signal for one of the six performed spontaneous fermentation processes of the *Agave* syrup (under the same experimental conditions) which was obtained by rebuilding from the redox potential data through the ANN procedure. The redox signal is displayed in (b). The maxima lines of the continuous wavelet transform of the biomass signal are shown in (c), of the transformed redox signal in (d), and in (e) one can see a comparison of their locations. (f) The corresponding $\tau(q)$ spectrum. (g) The multifractal singularity spectrum $f(\alpha)$ of the biomass and redox signals of this *Agave* spontaneous fermentation process.

singularity spectra for them, which indeed is the case. A detailed mapping of these Hölder irregularities to the metabolic parameters awaits more experimental data processed through the multifractal procedure. In the literature one can find that many other natural processes have been approached by the multifractal means, such as the membrane ion activity of K_{Ca} channels, i.e., their non-stationary dwell time series [16], the atmospheric energy cascades [17], and the point rainfall time series [18], to name just a few. In the well-established multifractal techniques one can find embedded a useful amount of information and we strongly believe that the wavelet multifractal computational scheme may provide an appropriate tool for quality control for this kind of spontaneous processes. The results of this paper together with our previous research on mixed growth [1] show that the wavelet methods are a very useful tool for detecting physical singularities in the fermentation processes.

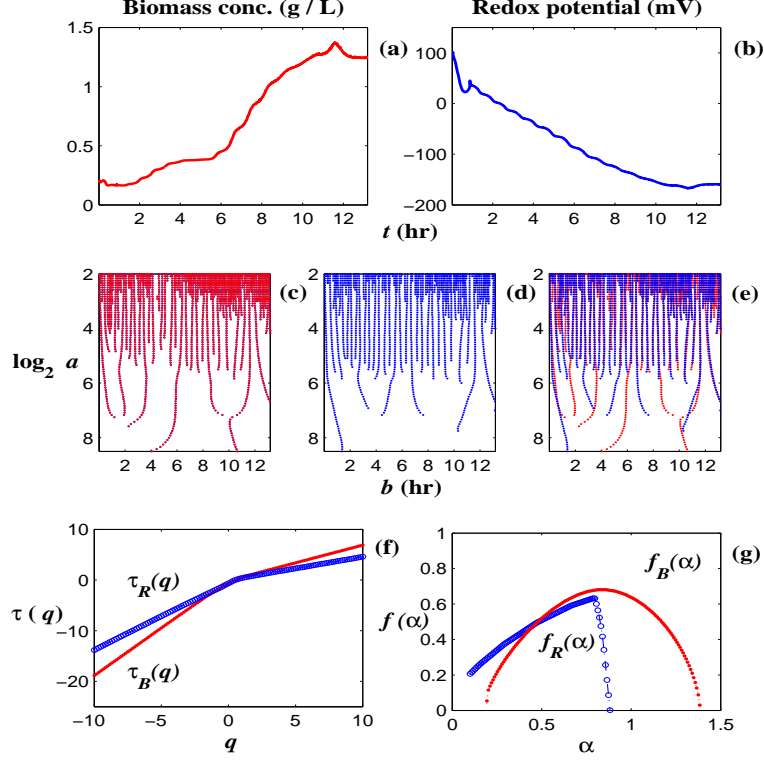


Fig. 3. (a) Biomass signal for another of the six spontaneous fermentation processes of the *Agave* syrup that we performed by rebuilding it through the ANN from the redox potential data (same experimental conditions) presented in (b). The redox signal is displayed in (b). The maxima lines of the continuous wavelet transform of the biomass signal are shown in (c), of the transformed redox signal in (d), and in (e) one can see a comparison of their locations. (f) The corresponding $\tau(q)$ spectrum. (g) The multifractal singularity spectrum $f(\alpha)$ of the biomass and redox signals of this *Agave* spontaneous fermentation process.

Acknowledgements

VIJ received partial financial support from PROMEP, JSM received partial financial support from PROMEP and FAI-UASLP. HCR has been partially supported through the CONACyT project 46980.

References

- [1] V. Ibarra-Junquera, P. Escalante-Minakata, J.S. Murguía, H.C. Rosu, Inferring mixed-culture growth from total biomass data in a wavelet approach, *Physica A*, 370 (2006) 777–792.
- [2] S.C.W. Kwong, L. Randers, R. Govin, On-line assessment of metabolic activities based on culture redox potential and dissolved oxygen profiles during aerobic fermentation, *Biotechnol. Prog.* 8 (1992) 576–579.
- [3] M. Berovič, Scale-up of citric acid fermentation by redox potential control, *Biotech. and Bioeng.* 64 (1999) 552–557.
- [4] C. van Dijk, T. Ebbenhorst-Selles, H. Ruisch, T. Stolle-Smits, E. Schijvens, W. van Deelen, C. Boeriu, Product and redox potential analysis of Sauerkraut fermentation, *J. Agric. Food Chem.* 48 (2000) 132–139.
- [5] N. Cheraiti, S. Guezenc, J.M. Salmon, Redox interactions between *Saccharomyces cerevisiae* and *Saccharomyces uvarum* in mixed culture under enological conditions, *Appl. Environmental Microbiol.* 71 (2005) 255–260.
- [6] A. Kukec, M. Berovič, S. Čelan, M. Wondra, The role of on-line redox potential measurement in *Sauvignon blanc* fermentation, *Food Technol. Biotechnol.* 40 (2002) 49–55.
- [7] T.C. Halsey, M.H. Jensen, L.P. Kadanoff, I. Procaccia, B.I. Shraiman, Fractal measures and their singularities: The characterization of strange sets, *Phys. Rev. A* 33 (1986) 1141–1151.
- [8] J.F. Muzy, E. Bacry, A. Arneodo, Wavelets and multifractal formalism for singular signals: Applications to turbulence data, *Phys. Rev. Lett.* 67 (1991) 3515–3518.
- [9] J.F. Muzy, E. Bacry, A. Arneodo, The multifractal formalism revisited with wavelets, *Int. Journal of Bifurcations and Chaos* 4 (1994) 245–302.
- [10] E. Bacry, J.F. Muzy, A. Arneodo, Singularity spectrum of fractal signals from wavelet analysis: Exact results, *J. Stat. Phys.* 70 (1993) 635–674.
- [11] J. S. Murguía, J. Urías, On the wavelet formalism for multifractal analysis, *Chaos* 11 (2001) 858–863.
- [12] A.S. Lapedes, R.M. Farber, Nonlinear signal processing using neural networks: Prediction and system modeling, Los Alamos Report LA-UR-87 (1987) 2662.
- [13] D. Rumelhart, J. McClelland, *Parallel Distributed Processing: Explorations in Microstructure of Cognition*, Vol. 1, Foundations, MIT Press, Cambridge, MA., 1986, pp. 318–362.
- [14] S. Mallat, W.L. Hwang, Singularity detection and processing with wavelets, *IEEE Trans. Inform. Theory* 38(2) (1992) 617–643.

- [15] A. Humeau, F. Chapeau-Rousseau, M. Tartas, B. Fromy, P. Abraham, Multifractality in the peripheral cardiovascular system from pointwise Hölder exponents of laser Doppler flowmetry signals, *Biophys. J.* 93(12) (2007) L59-L61.
- [16] V.N. Kazachenko, M.E. Astashev, A.A. Grinevich, Multifractal analysis of K^+ channel activity, *Biochemistry (Moscow)* 1(2) (2007) 169-175.
- [17] S. Lovejoy, D. Schertzer, J.D. Stanway, Direct evidence of multifractal atmospheric cascades from planetary scales down to 1 km, *Phys. Rev. Lett.* 86(22) (2001) 5200-5203.
- [18] H. Bendjoudi, P. Hubert, D. Schertzer, Multifractal point of view on rainfall intensity-duration-frequency curves, *C. R. Acad. Sci. Paris II* 325 (1997) 323-326.